X-ray Detector Simulation Pipelines for the European XFEL

Tonn Rüter, Steffen Hauf, Markus Kuster, Ashley Joy, Ruth Ayers, Matthew Wing, Chun Hong Yoon, and Adrian P. Mancuso

***Abstract*—The European X-ray Free Electron Laser is a high-intensity X-ray light source currently being constructed in the Hamburg region that will provide spatially coherent X-rays in the energy range between 0.25 keV – 25 keV. The LPD, DSSC and AGIPD detectors are being developed to provide megapixel imaging capabilities with a dynamic range spanning from single photon sensitivity to 10^5 photons per pixel. Calibration of these detectors is challenging as a large set of calibration parameters (up to 10^9) exist. To provide a drop-in replacement for measured megapixel detector data, the X-ray Camera Simulation Toolkit (X-CSIT) has been developed. Based on X-CSIT, a X-ray detector simulation pipeline (XDSP) has been assembled to simulate a realistic detector response at a given experimental configuration. Validation of XDSPs have been performed and an XDSP for the SPB/SFX imaging experiment based on calibration data of an AGIPD module has been implemented and integrated into the experiment's start-to-end simulation framework simS2E.**

I. Introduction

THE European X-ray Free Electron Laser [1] is a high-intensity X-ray light source currently being constructed in the Hamburg region in Germany, that will provide spatially coherent X-rays in the energy range between $0.25\,\mathrm{keV}$ and $25\,\mathrm{keV}$. The machine will deliver a unique time structure, consisting of up to $2700\,\mathrm{pulses}$, with a $4.5\,\mathrm{MHz}$ repetition rate, 10 times per second at very high photon fluxes up to 10^{13} photons per pulse [2]. The LPD [3, 4], DSSC [5, 6] and AGIPD [7] detectors are being developed to provide megapixel imaging capabilities at the aforementioned repetition rates for a dynamic range spanning from single photon sensitivity to 10^4 – 10^5 photons per pixel. The detectors are optimized for specific energy ranges.

II. Motivation

Calibration of these detectors is challenging as a large set of calibration parameters (up to 10^9) exists. In order to aid in calibration and, at a later stage, provide users with a possibility of accurately simulating a detector's response for a given set of experimental conditions, the X-ray Camera Simulation Toolkit (X-CSIT, [8]) is being developed at European XFEL in collaboration with University College London. The simulation toolkit needs to be able to accommodate the variety of possible detectors and the diverse experimental environments in which they will work in. X-CSIT provides this flexibility. For a seamless interplay of X-CSIT with the European XFEL's data processing pipelines and calibration database it has been integrated into to the XFEL's Karabo framework [9], thereby also making X-CSIT available as a drop-in replacement for measured detector data. Within the Karabo framework, individual simulations for X-ray/matter interaction (handled by Geant4 [10, 11]), charge carrier transport and the influence of the detector's ASIC on the signal can be combined to create a X-ray Detector Simulation Pipeline (XDSP). XDSPs will allow users of the European XFEL to anticipate the influence of the detector on the measurement signal and their data processing pipelines and thus allow for optimization of parameters of the detector configuration such as tilt, roll, position, gap opening and gain.

T. Rüter, S. Hauf, M. Kuster, A. P. Mancuso are with the European XFEL GmbH, Hamburg, Germany. E-mail: tonn.rueter@xfel.eu.

A. Joy and R. Ayers are with University College London, London, UK.

M. Wing is with University College London, London, UK and Deutsches Elektronen Synchrotron (DESY), Hamburg, Germany.

C. Hong Yoon is with the SLAC Linac Coherent Light Source (LCLS), Menlo Park, CA, USA

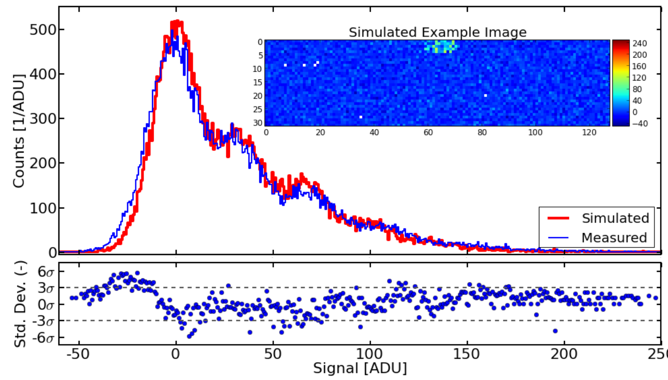

Figure 1: *Comparison of spectra of simulated and measured pencil beam images from a LPD prototype tile. Residuals in terms of* 1σ *experimental uncertainties are shown. Inset: single simulated image after offset and common-mode corrections.*

III. Initial validation

The validation of X-CSIT is of crucial importance. Results of initial validation for a XDSP simulating s flat field measurement on a pnCCD detector with an Fe55–source have been published in [8]. Due to its small pixels size ($75\,\mu\mathrm{m}^2$), the pnCCD detector serves as a testbed for the validation of our charge simulation. A comparison of the raw simulated and measured datasets shows a 3σ agreement between both. Further analysis of the datasets focused on charge sharing effects, which occur when the charge generated by an event (e.g. an incident photon) is registered in two or more pixels. The simulated dataset confirms higher numbers of events in which charge was shared across 3- and 4-pixel events while

Properties	LPD	pnCCD	AGIPD
Pixel size	500 μm square	75 μm square	200 μm square
Thickness	500 μm	450 μm	500 μm
Dynamic range	10^5 at 12 keV	10^3 at 2 keV, 130 eV at 5.9 keV	10^4 at 12 keV
Dyn. range technique	Triple gain profile	Linear	Preamplifier chosen gain
Sensor size	32×128 pixels	200×128 pixels	512×128 pixels
Photon energy range	$1 - 24$ keV	$0.1 - 15$ keV	$3 - 13$ keV

Table I: *Technical specifications of the European XFEL detectors discussed in this work.*

1- and 2-pixel events had lower numbers. We attribute this to a too large charge cloud, the cause for which remains under investigation.

Additional validation was performed for a single tile of the LPD detector. The tile was partially irradiated by a monochromatic, attenuated and collimated 12 keV beam at the Diamond Synchrotron. The images were recorded using the synchrotron's hybrid mode, allowing the LPD to run at 4.5 MHz. Fig. 1 shows spectra of simulated and measured data after offset and common mode corrections have been applied; the inset shows an exemplary simulated image. Notice the partial direct beam in the upper middle part of the image. Measurement and simulation show an agreement within $3-5\,\sigma$ depending on region. In the spectra of both the simulated and the measured data set we can identify the noise peak as well as single, double and triple photon peaks. The simulations were performed such that the number of simulated events matches the experimental conditions. Thus, both measured and simulated spectra in Fig. 1 show absolute numbers and are not normalized. An overview of the characteristics of the detectors referred to in this paper can be found in Tab. I.

IV. Example use case: SPB/SFX simS2E

Currently, the use case of experiment optimization is evaluated in the context of the Single Particle and Biomolecule/Serial Femtosecond Crystallography (SPB/SFX) imaging instrument [12], which is under construction at the European XFEL. SPB/SFX is developing a start-to-end simulation framework, simS2E [13], that allows users to simulate every stage of a single particle experiment: the amplification of XFEL source, propagation through optics, X-ray/matter interaction, coherent diffraction, detector response and reconstruction. A XDSP has been integrated simulate a realistic detector response and its effect on the subsequent reconstruction as is shown in Fig. 3. First data using an XDSP simulating an AGIPD module's response at 5 keV has been successfully generated. Production of simulated dark images is demonstrated by the spectra calculated from simulated and measured dark image data shown in Fig. 2, where agreement is within $3\,\sigma$ uncertainties of the measured data. The inset depicts a single, simulated dark frame of an AGIPD Module. A gain map was produced by interpolation calibration data for 12.4 keV.

The SPB/SFX use case is interesting for two reasons: While the reconstruction algorithms are noise-robust, the measurement signals are extremely sparse. In the photon counting regime, detector noise becomes important, especially concerning the occurrence of false positives. First qualitative comparisons of re-orientation results using the Expand-Maximize-Compress (EMC) algorithm [14] are shown in Fig. 4. For this comparison an AGIPD quadrant was simulated to measure diffraction images of nitrogenase iron protein (2NIP) at 5 keV – the lower end of its design energy-range. Data was rebinned to 64×64 pixels for analysis (81×81 for the ideal detector). From left to right maximum density projections of the reoriented diffraction volume are shown for an ideal detector, the simulated AGIPD with simple analysis, i.e. rounding to the next integer photon count and a probabilistic analysis. In the latter case the probability of an event belonging to a given incident photon intensity I_{k} is evaluated using knowledge about the detector's counting uncertainty for photon number k and noise σ as

$$I_{\mathrm{k}} = \frac{k p_{\mathrm{k}}}{\sum_{i=0}^{N_{\mathrm{peak}}} p_{\mathrm{i}}} \tag{1}$$

with

$$p_{\mathrm{k}} = A_{\mathrm{k}} \exp\left(\frac{I - gk}{2\sigma_k^2}\right), \tag{2}$$

where N_{peak} is the number of evaluated photon peaks, A_{k} and σ_{k} are the peak amplitude and standard deviation as determined by fitting Gaussian peaks to the total event spectrum of the simulated data, and g is the conversion gain of the detector, converting a photon number k to a signal in keV or ADU. An event is recorded if the evaluated pixel intensity surpasses an event threshold $T_{\mathrm{E}} = 0.5$ and the probability of the event being due to detector noise is $p_0 < 10^{-5}$.

Qualitatively, it is apparent from the figure that detector noise and false positives make orientation using only a simple analysis impossible. Using the probabilisitic analysis noise is largely suppressed and features start to reappear. A quantitative analysis is currently in preparation and will be published at a later time.

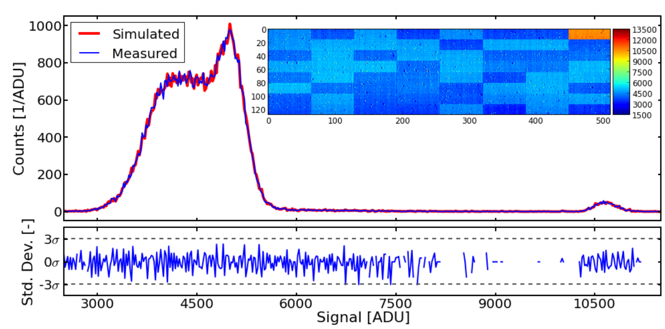

Figure 2: *Comparison of spectra of simulated and measured dark images from an AGIPD prototype module. Residuals in terms of 1σ experimental uncertainties are shown. Inset: single simulated image.*

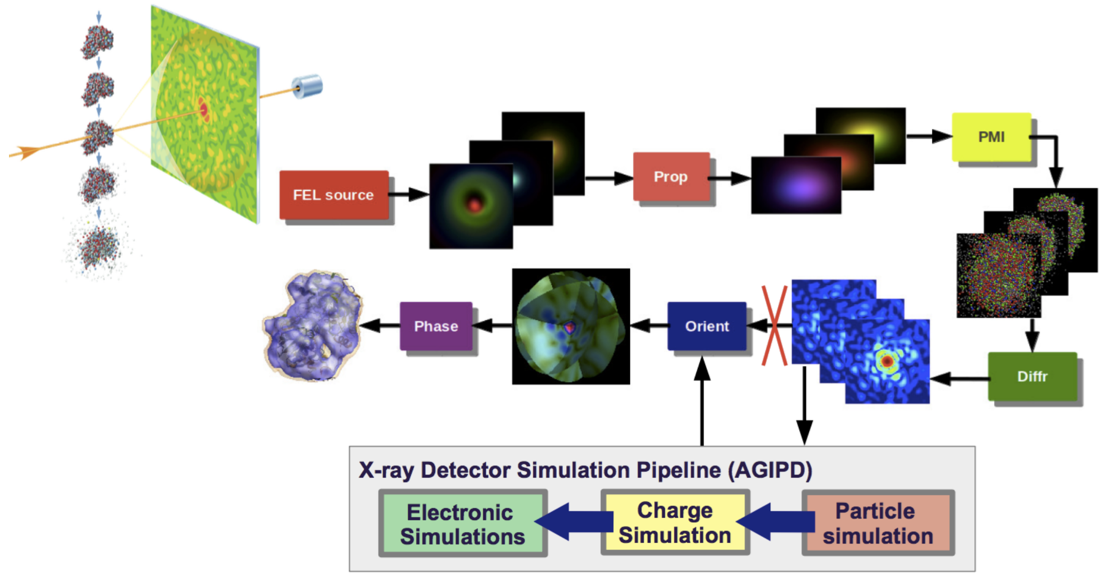

Figure 3: *Overview of simS2E simulation pipeline and where XDSP's hook into the simulation, providing an realistic estimate of detector performance.*

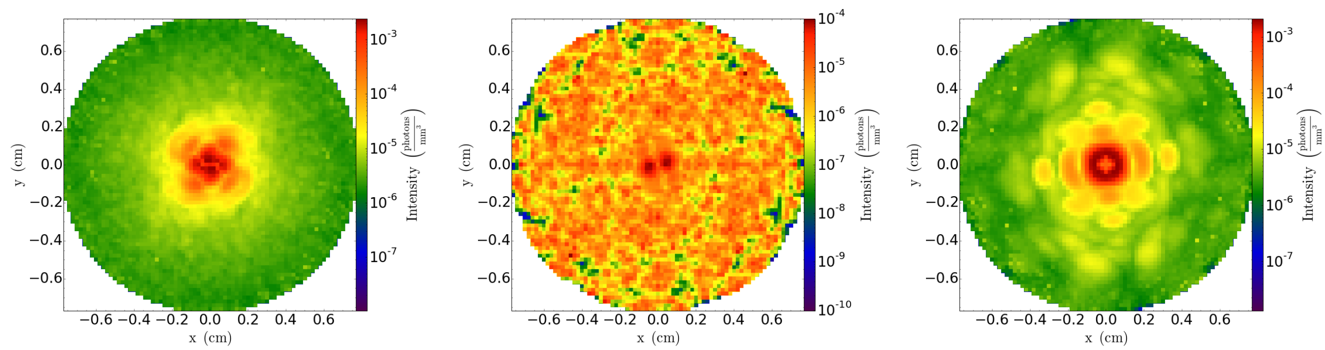

Figure 4: *Comparison of EMC orientation results in terms of maximum density projections of a 2NIP molecule for an ideal detector (left panel), a simulated AGIPD quadrant using simple (middle panel) and probabilistic analysis methods (right panel, see text).*

V. Conclusion

We have presented validation aspects of a X-ray detector simulation pipeline (XDSP) for the 2D semiconductor detectors at the European XFEL. It was shown that XDSPs allow simulation of realistic detector responses for the pnCCD, LPD and AGIPD detectors within $5\,\sigma$ uncertainties on the measured data. In the use-case of the SPB instrument's start-to-end-simulation (simS2E) seamless integration into the XFEL data processing chain was shown and the need for a realistic detector simulation was highlighted by contrasting re-orientation results with an ideal detector.

VI. Acknowledgments

The authors would like to thank the AGIPD Consortium for providing the calibration data necessary for our simulation of the AGIPD dark frames and Philipp Lang and the LPD consortium for providing the experimental data concerning the LPD simulation. M. Wing acknowledges the support of the Alexander von Humboldt Foundation.

References

[1] M. Altarelli, "The European X-ray free-electron laser," European XFEL GmbH, Tech. Rep. July, 2006.
[2] T. Tschentscher, "Layout of the X-Ray Systems at the European XFEL," European XFEL GmbH, Tech. Rep. April, 2011.
[3] M. Hart *et al.*, "Development of the LPD, a high dynamic range pixel detector for the European XFEL," *2012 IEEE Nuclear Science Symposium and Medical Imaging Conference Record (NSS/MIC)*, pp. 534–537, Oct. 2012.
[4] A. Koch *et al.*, "Performance of an LPD prototype detector at MHz frame rates under Synchrotron and FEL radiation," *Journal of Instrumentation*, vol. 8, no. 11, pp. C11 001–C11 001, Nov. 2013.
[5] M. Porro *et al.*, "Expected performance of the DEPFET sensor with signal compression: A large format X-ray imager with mega-frame readout capability for the European XFEL," *Nuclear Instruments and Methods in Physics Research Section A: Accelerators, Spectrometers,*

Detectors and Associated Equipment, vol. 624, no. 2, pp. 509–519, 2010.

[6] G. Lutz, P. Lechner, M. Porro, L. Strüder, and G. De Vita, "DEPFET sensor with intrinsic signal compression developed for use at the XFEL free electron laser radiation source," *Nuclear Instruments and Methods in Physics Research, Section A: Accelerators, Spectrometers, Detectors and Associated Equipment*, vol. 624, no. 2, pp. 528–532, 2010.

[7] H. Graafsma, "Requirements for and development of 2 dimensional X-ray detectors for the European X-ray Free Electron Laser in Hamburg," *Journal of Instrumentation*, vol. 4, no. 12, pp. P12 011–P12 011, 2009.

[8] A. Joy, M. Wing, S. Hauf, M. Kuster, and T. Rüter, "X-CSIT: A Toolkit for Simulating 2D Pixel Detectors," *Journal of Instrumentation*, vol. 10, no. C04022, 2015.

[9] B. C. Heisen *et al.*, "Karabo : an Integrated Software Framework Combining Control, Data Management, and Scientific Compution Tasks," in *ICALEPCS2013: Proceedings of the 14th International Conference on Accelerator & Large Experimental Physics Control Systems*, 2014, pp. 1465–1468.

[10] S. Agostinelli *et al.*, "GEANT4 - A simulation toolkit," *Nuclear Instruments and Methods in Physics Research, Section A: Accelerators, Spectrometers, Detectors and Associated Equipment*, vol. 506, no. 3, pp. 250–303, 2003.

[11] J. Allison *et al.*, "Geant4 developments and applications," *IEEE Transactions on Nuclear Science*, vol. 53, no. 1, pp. 270–278, 2006.

[12] A. P. Mancuso, "Scientific Instrument Single Particles, Clusters, and Biomolecules (SPB)," European XFEL GmbH, Tech. Rep., 2012.

[13] C. H. Yoon, M. V. Yurkov, E. A. Schneidmiller, L. Samoylova, A. Buzmakov, Z. Jurek, R. Santra, N. D. Loh, T. Tschentscher, and A. P. Mancuso, "simS2E : A multi-physics framework for modelling a complete single particle imaging experiment at an X-ray Free Electron Laser," *In Preparation*, pp. 1–43, 2015.

[14] N.-T. D. Loh and V. Elser, "Reconstruction algorithm for single-particle diffraction imaging experiments," *Physical Review E*, vol. 80, no. 2, p. 026705, 2009.